

ELECTRONIC SUPPORTING INFORMATION

Julien Massue,^{a*} Abdellah Felouat,^a Pauline M. Vérité,^b Denis Jacquemin,^{b*}
Konrad Cyprych,^c Martyna Durko,^c Lech Sznitko,^c Jaroslaw Mysliwiec^{c*} and
Gilles Ulrich^{a*}

E-mail: massue@unistra.fr, Denis.Jacquemin@univ-nantes.fr, gulrich@unistra.fr,
jaroslaw.mysliwiec@pwr.edu.pl

Scheme S1. Preparation of HBO 1.

Figure S1 ¹H NMR spectrum of HBO 1

Figure S2 ¹³C NMR spectrum of HBO 1

Figure S3 HR-MS spectrum

Figure S4 Absorption, emission and excitation spectra of HBO 1 in toluene

Figure S5 Absorption, emission and excitation spectra of HBO 1 in ethanol

Figure S6 Emission and excitation spectra of HBO 1 in potassium bromide pellets

Figure S7 Emission and excitation spectra of HBO 1 as 1% in PMMA films

Table S1. Photophysical properties of HBO 2

Figure S8 Absorption, emission and excitation spectra of HBO 2 in toluene

Figure S9 Absorption, emission and excitation spectra of HBO 2 in ethanol

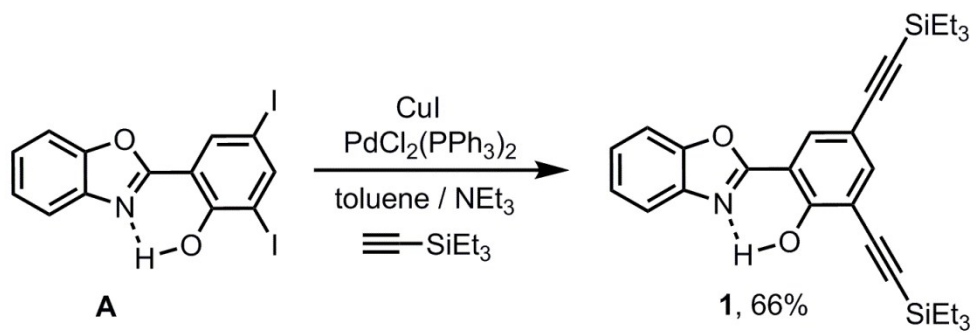
Figure S10 Emission and excitation spectra of HBO 2 in potassium bromide pellets

Figure S11 Optical microscope images of samples used for RL emission measurements
(fluorescence mode).

Figure S12 Emission and RL emission spectra with indicated values of FWHM

Theoretical methods

References



Scheme S1. Preparation of HBO dye **1**.

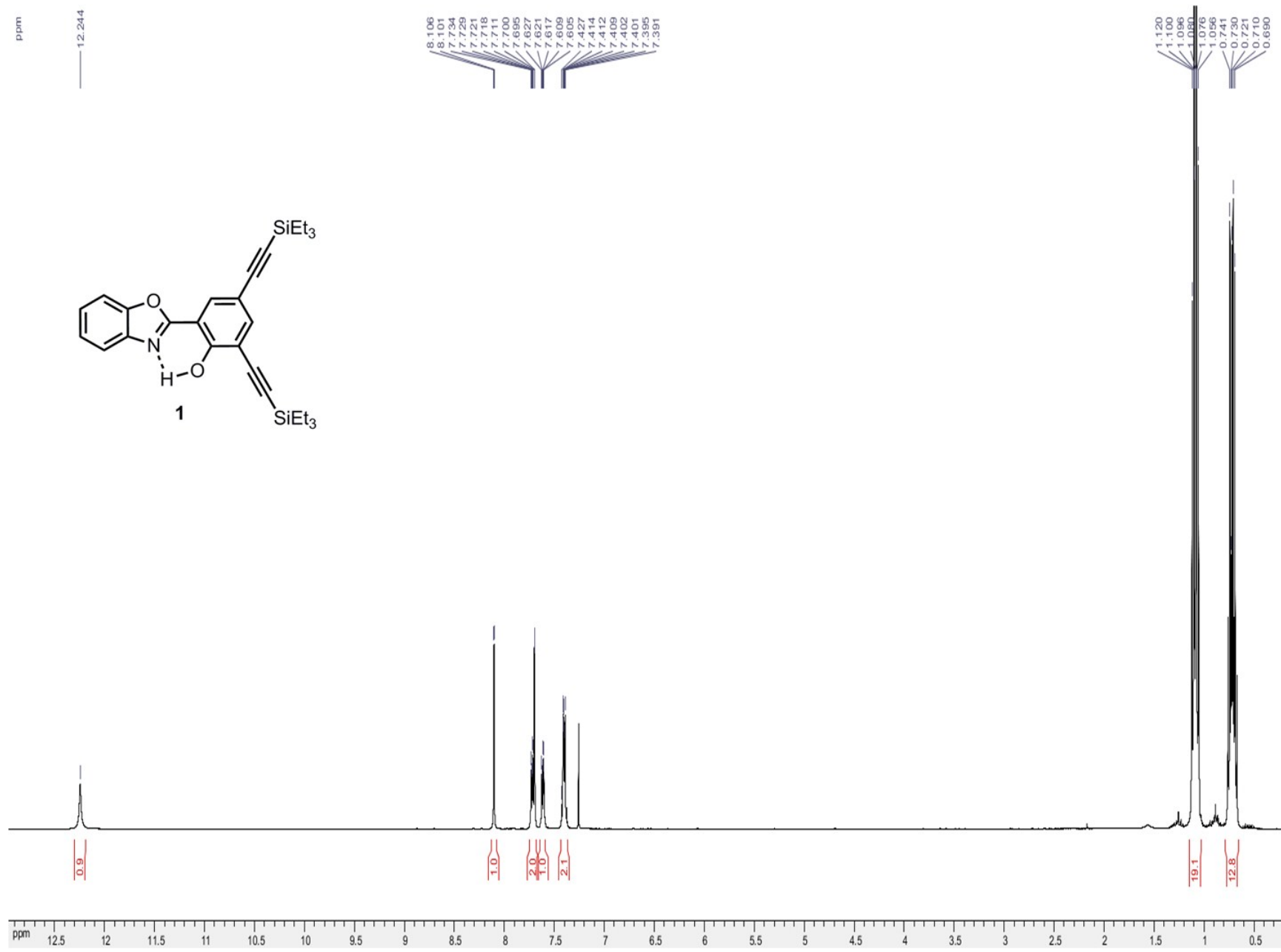


Figure S1 ^1H NMR spectrum of HBO 1

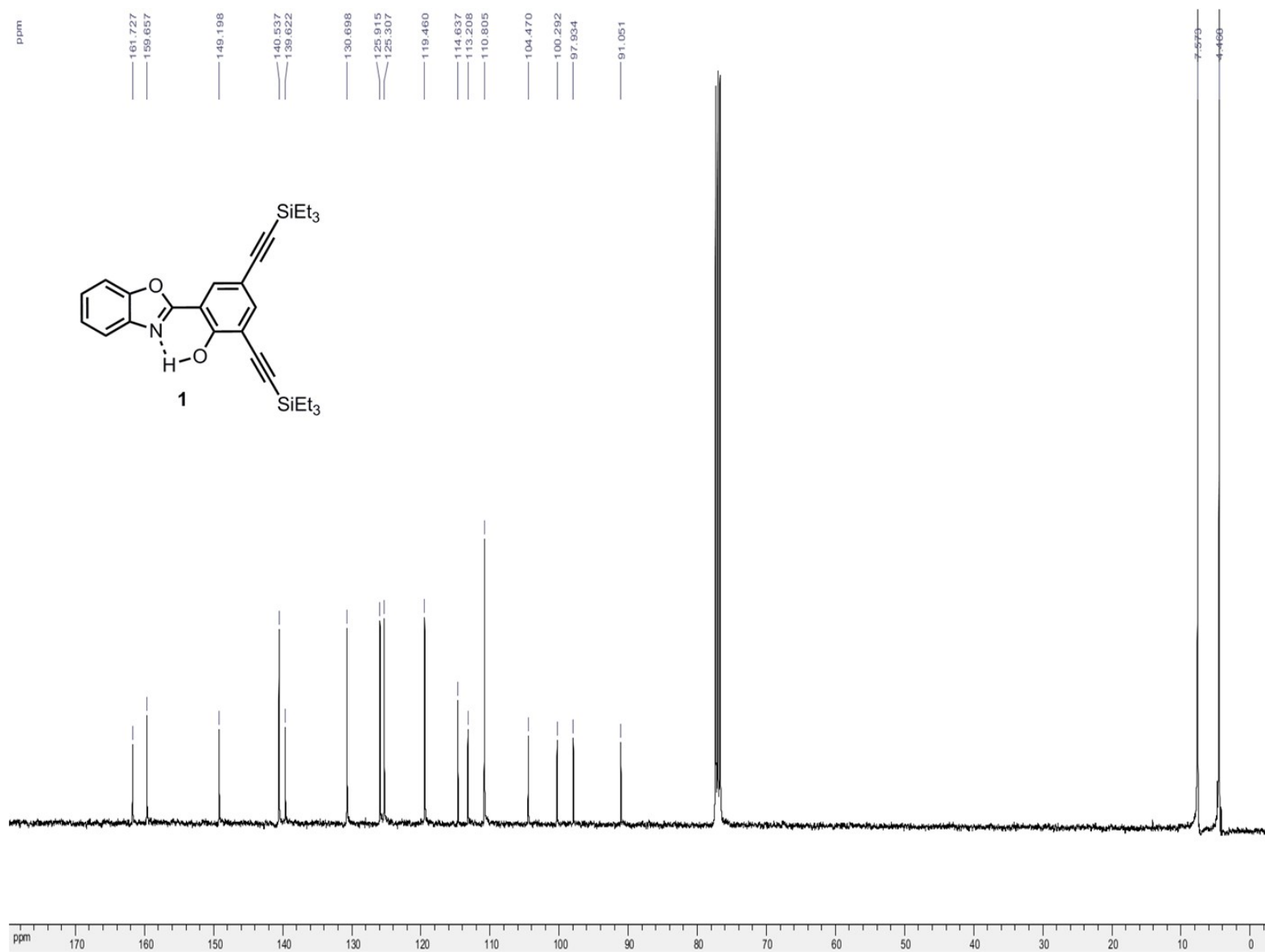
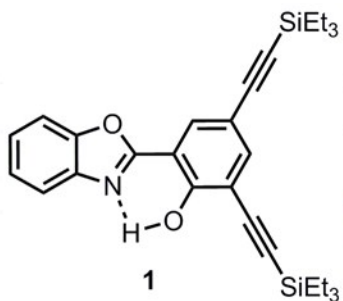


Figure S2 ¹³C NMR spectrum of HBO 1



Mass Spectrum Molecular Formula Report

Service masse 2017\O41805SK.d
pos.m

Acquisition Date 3/10/2017 9:47:50 AM

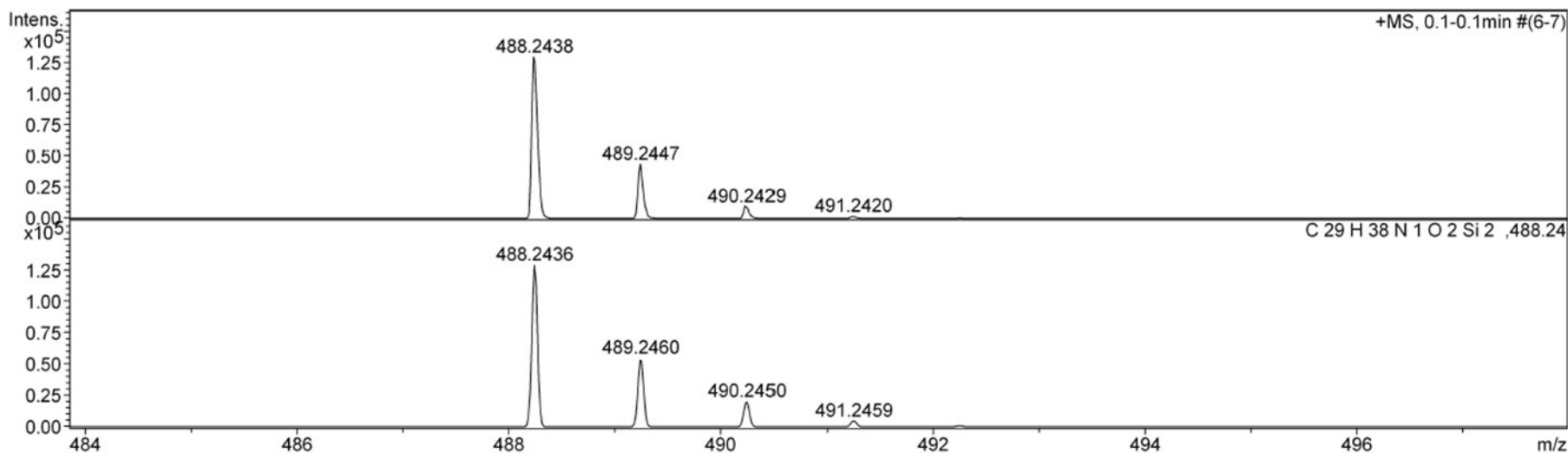
Operator Administrator
Instrument micrOTOF 66

Acquisition Parameter

Source Type ESI
Scan Range n/a
Scan Begin 50 m/z
Scan End 3000 m/z

Ion Polarity Positive
Capillary Exit 150.0 V
Hexapole RF 220.0 V
Skimmer 1 50.0 V
Hexapole 1 24.3 V

Set Corrector Fill 57 V
Set Pulsar Pull 811 V
Set Pulsar Push 811 V
Set Reflector 1700 V
Set Flight Tube 8600 V
Set Detector TOF 1950 V



Sum Formula	Sigma	m/z	Err [ppm]	Mean Err [ppm]	rdb	N Rule	e ⁻
C 29 H 38 N 1 O 2 Si 2	0.06	488.2436	-0.40	1.11	13.50	ok	even
C 29 H 37 N 1 O 2 Si 2	0.58	487.2357	-11.46	-12.08	14.00	-	odd

Figure S3 HR-MS spectrum of HBO 1

Figure S4 Absorption, emission and excitation spectra of HBO 1 in toluene at 25°C

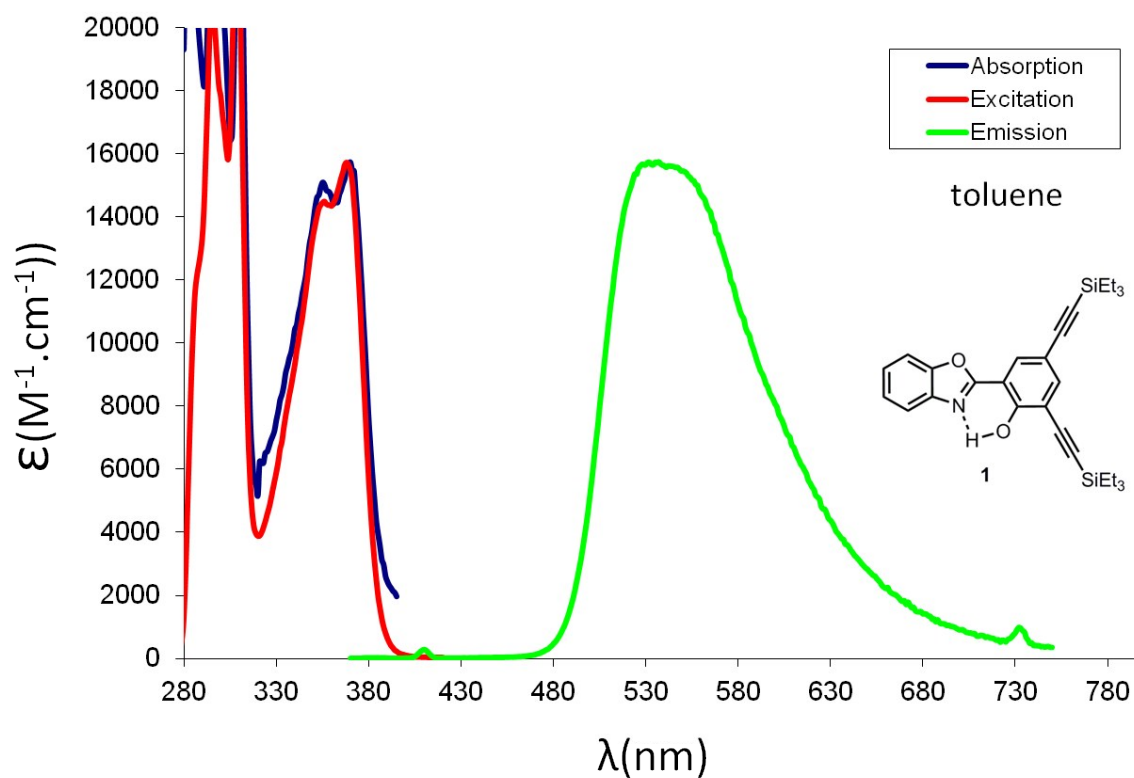


Figure S5 Absorption, emission and excitation spectra of HBO 1 in ethanol at 25°C

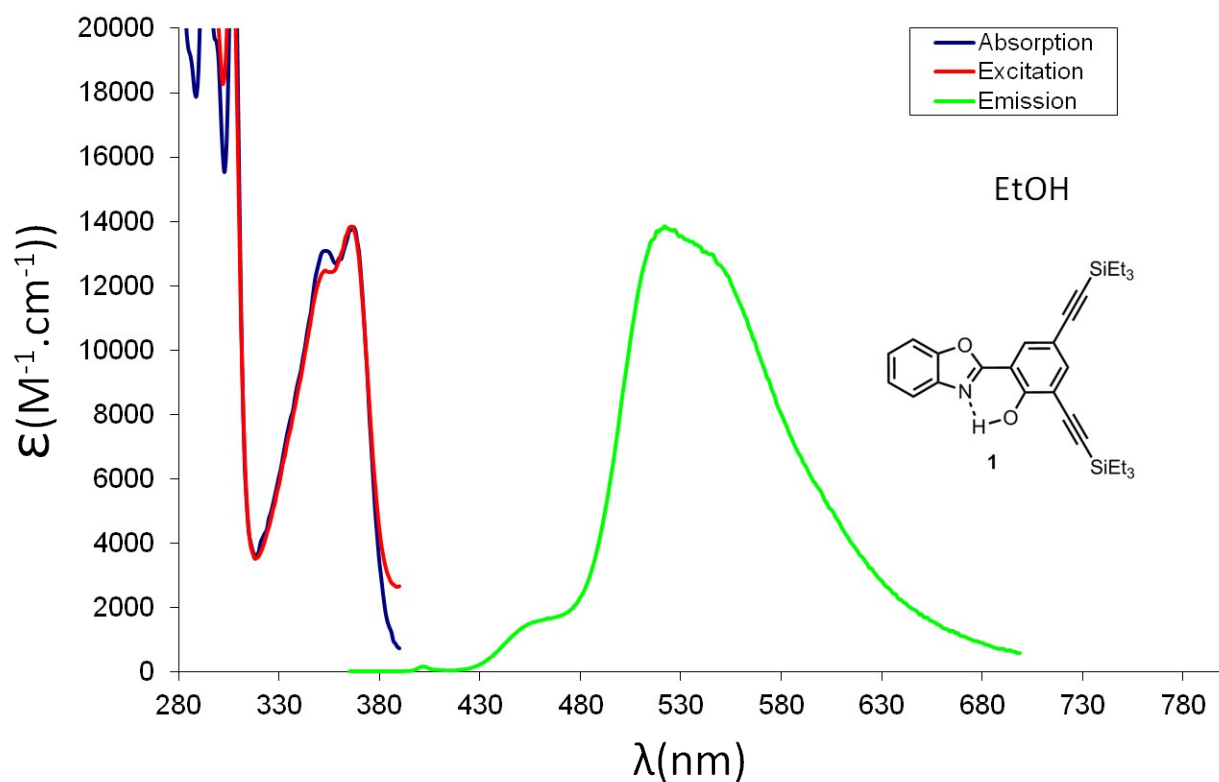


Figure S6 Emission and excitation spectra of HBO **1** in potassium bromide pellets (concentration around 10^{-5} M)

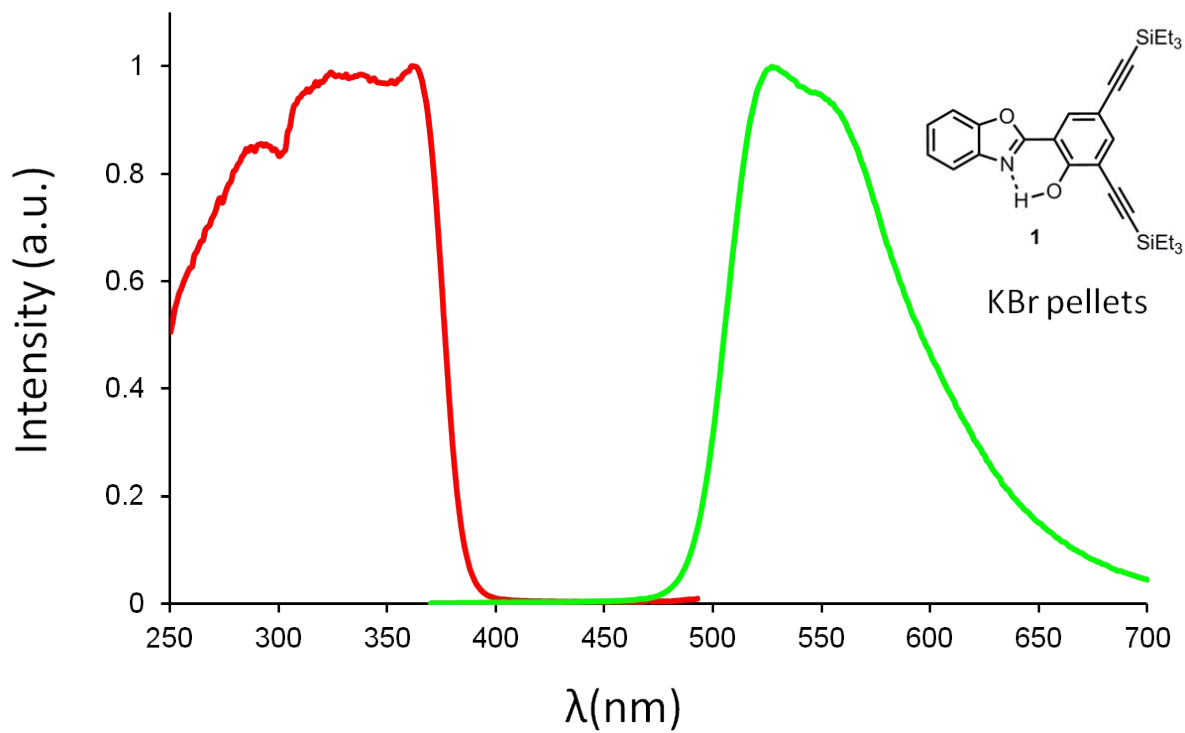


Figure S7 Emission and excitation spectra of HBO **1** as 1% in PMMA films

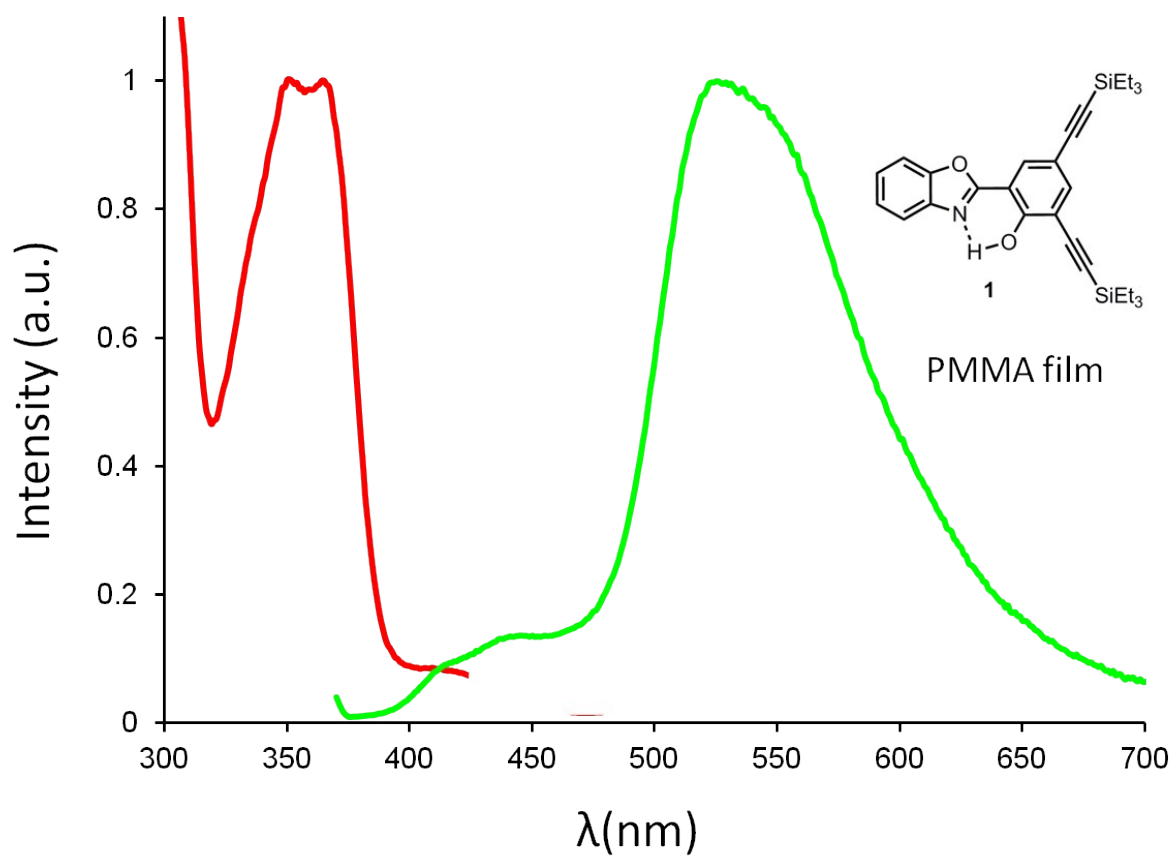


Table S1. Photophysical properties of HBO 2

$\lambda_{\text{abs}}^{[\text{a}]}$ (nm)	$\epsilon^{[\text{b}]}$ ($\text{M}^{-1} \cdot \text{cm}^{-1}$)	$\lambda_{\text{em}}^{[\text{c}]}$ (nm)	$\Delta S^{[\text{d}]}$ (cm^{-1})	$\Phi_{\text{F}}^{[\text{e}]}$	$\sigma^{[\text{f}]}$ (ns)	K_{r} (10^8s^{-1}) ^[g]	K_{nr} (10^8s^{-1}) ^[g]	Solvent/ Matrix
321	23100	406/490	6500	0.02	3.6	0.06	2.72	Toluene
317	20800	397/481	6400	0.01	2.8	0.04	3.54	EtOH
363	-	498	7500	0.17	-	-	-	KBr

^[a] Wavelength of absorption (solution) or excitation (solid-state) maximum ^[b] Molar absorption coefficient ^[c] Maximum emission wavelength ^[d] Stokes' shift ^[e] Solution relative quantum yields determined by using Rhodamine 6G as a reference ($\lambda_{\text{exc}} = 488 \text{ nm}$, $\Phi = 0.88$ in ethanol) or solid-state absolute quantum yields determined using an integration sphere ^[f] Fluorescence lifetime ^[g] The fluorescence (K_{r}) and non radiative (K_{nr}) rate constants were calculated in toluene and ethanol using the following equations: $K_{\text{r}} = \Phi_{\text{F}}/\tau$ and $K_{\text{nr}} = (1-\Phi_{\text{F}})/\tau$.

Figure S8 Absorption, emission and excitation spectra of HBO 2 in toluene at 25°C

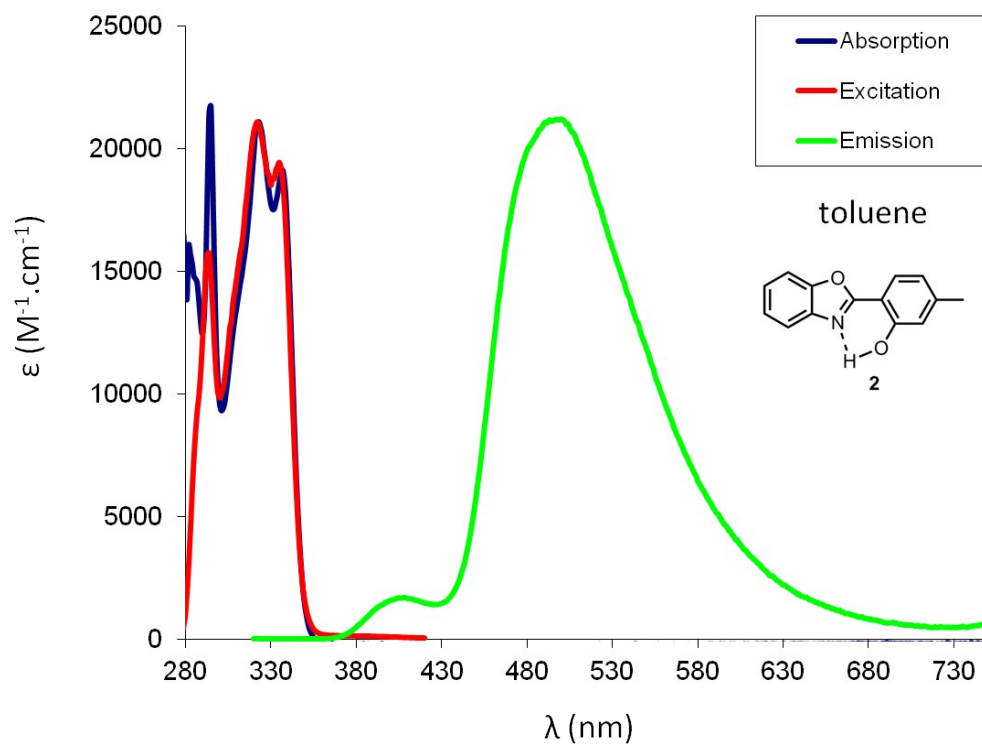


Figure S9 Absorption, emission and excitation spectra of HBO 2 in ethanol at 25°C

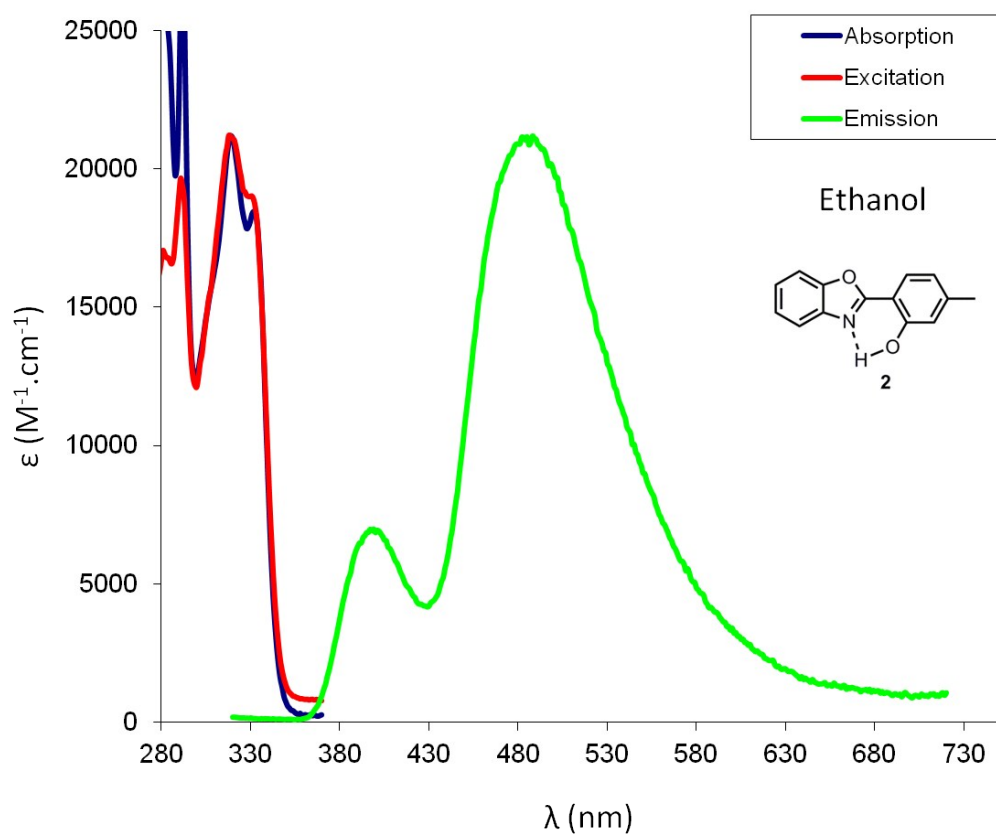


Figure S10 Emission and excitation spectra of HBO 2 in potassium bromide pellets (concentration around 10^{-5}M)

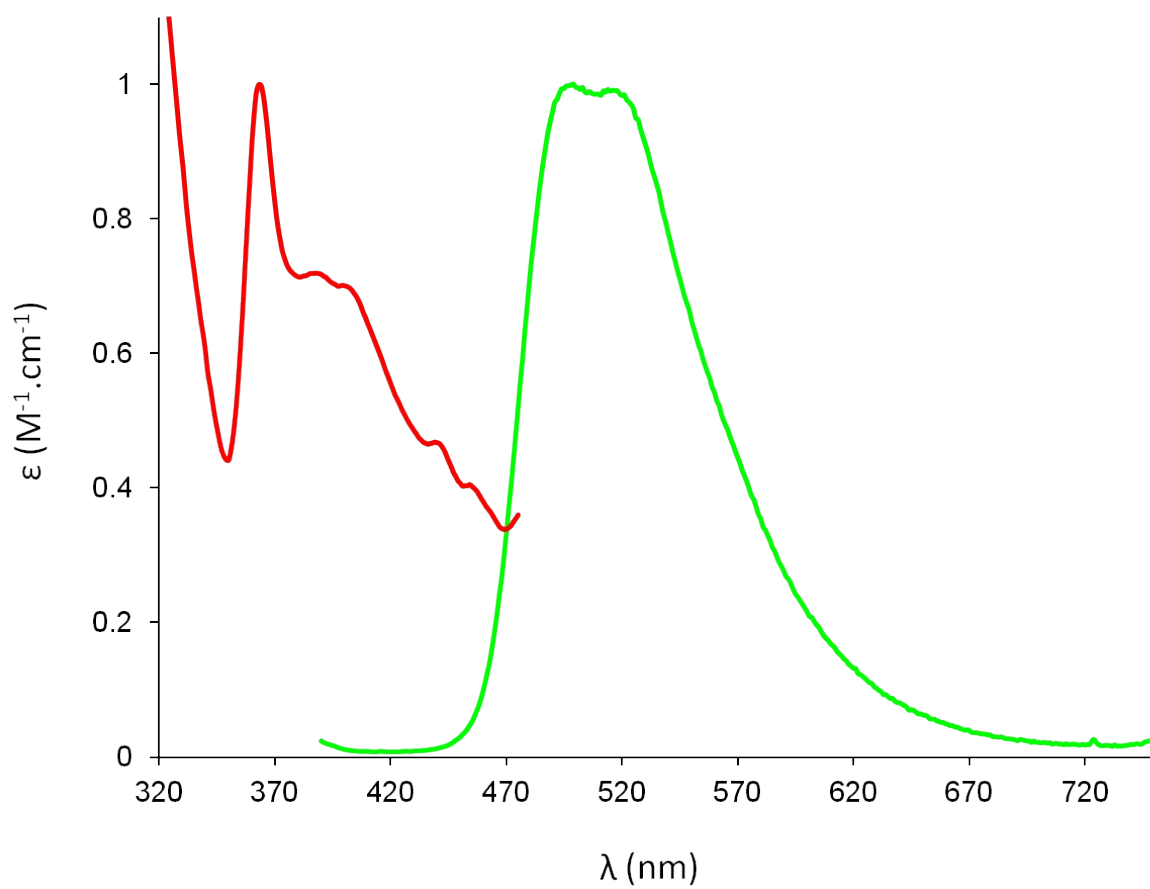


Figure S11 Optical microscope images of PMMA/HBO thin films and powder (final image) samples used for RL emission measurements (fluorescence mode).

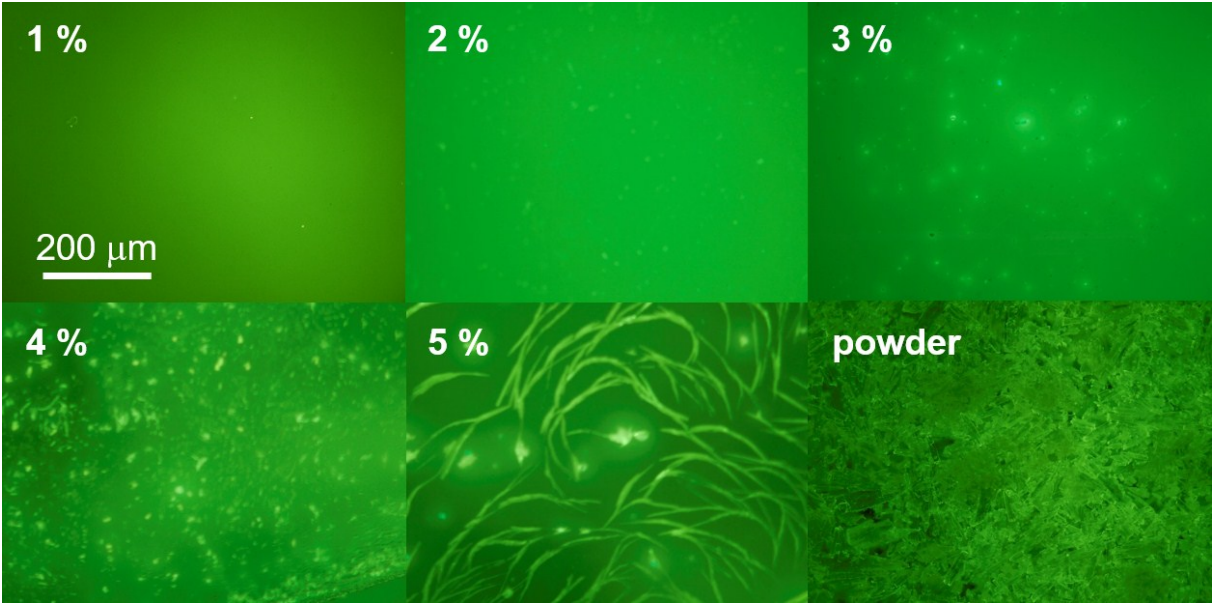
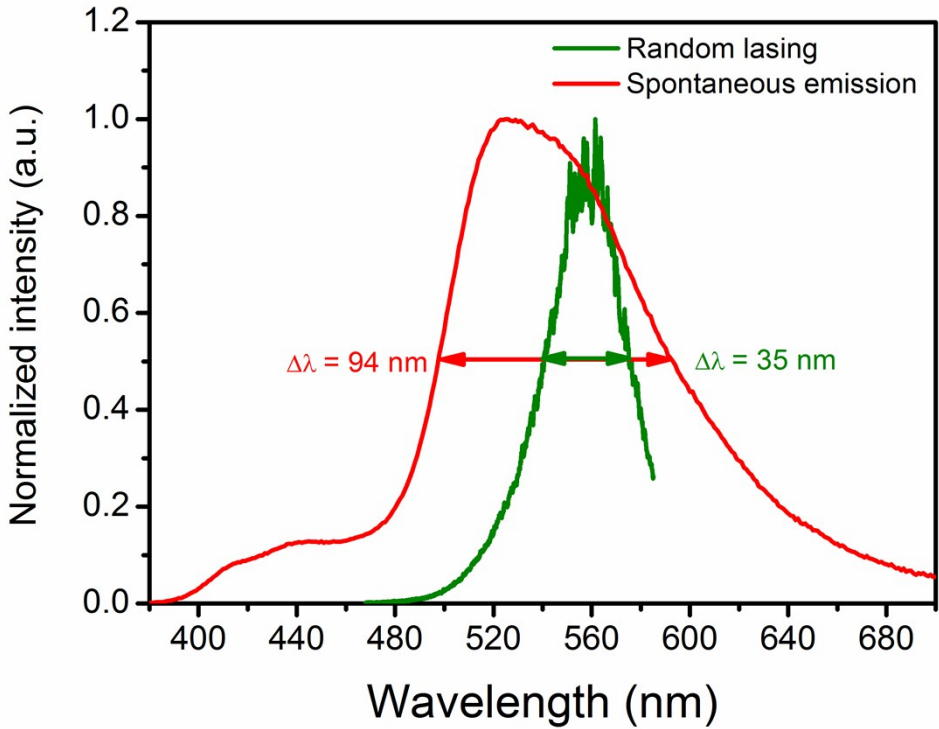


Figure S12 Emission and RL emission spectra with indicated values of FWHM



Theoretical methods

Our computational protocol is based on current state-of-the-art for modeling ESIPT-type reactions as well as the emission and absorption spectra of comparable types of molecules.¹ We used a composite approach combining the results of Time-Dependent Density Functional Theory (TD-DFT) and the second-order algebraic diagrammatic construction [ADC(2)] method. In this composite approach,^{2b} the structures and vibrations are determined by using (TD-)DFT geometries obtained with the M06-2X functional, the solvent effects are modeled with the polarizable-continuum model (PCM)² and the total and transition energies are corrected with ADC(2) to obtain theoretical best estimates. The ADC(2) calculations relied on the Resolution-of-Identity (RI) technique and were performed with default parameters. All DFT/TD-DFT calculations were performed by using Gaussian 16 software,³ whereas all ADC(2) calculations were performed by using Turbomole 6.6.⁴ For geometry optimizations, the compact 6-31G(d) atomic basis set has been used, whereas the extended 6-311+G(2d,p) [*aug-cc-pVTZ*] atomic basis set has been applied for TD-DFT [ADC(2)] transition-energy calculations. The optimized structure of ground and excited states were confirmed by frequency calculations by using analytical Hessian for both the ground and the excited states, which resulted in no imaginary frequency for E, E* and K*, and one imaginary frequency for the transition-state structure corresponding to the proton-transfer (TS*). To achieve numerical stability in the results, we used a tightened self-consistent field (10^{-10} a.u.) and geometry optimization (10^{-5} a.u.) convergence criteria and the so-called *ultrafine* (99,550) DFT-pruned integration grid in all our TD-DFT calculations. Geometry optimizations and Hessian calculations of the excited states took advantage of the linear-response (LR)⁵ PCM scheme whereas for transition energies the more elaborate corrected LR scheme (cLR)⁶ was used to take into account the change in the cavity polarization upon electron excitation by calculation of excited-state one-electron density. During gradient and Hessian TD-DFT calculations, we applied the *equilibrium* regime of PCM solvation (slow processes), absorption and fluorescence were treated as fast *nonequilibrium* processes. Toluene was used as solvent. The density difference plots ($\Delta\rho$) were obtained from the difference in the total density of the excited state and the ground state (LR-PCM-TD-DFT calculation), with the former calculated by using so-called Z-vector approach. A contour threshold of 0.008 au was used for the representation.

References

- (1) (a) M. Raoui, J. Massue, C. Azarias, D. Jacquemin, G. Ulrich, *Chem. Commun.* **2016**, 52, 9216–9219; (b) C. Azarias, S. Budzak, A. D. Laurent, G. Ulrich, D. Jacquemin, *Chem. Sci.* **2016**, 7, 3763–3774; (c) Y. Houari, S. Chibani, D. Jacquemin, A. D. Laurent, *J. Phys. Chem. B* **2015**, 119, 2180–2192; (d) M. Savarese, P. A. Netti, C. Adamo, N. Rega, I. Ciofini, *J. Phys. Chem. B* **2013**, 117, 16165–16173; (e) L. Wilbraham, M. Savarese, N. Rega, C. Adamo, I. Ciofini, *J. Phys. Chem. B* **2015**, 119, 2459–2466.
- (2) J. Tomasi, B. Mennucci, R. Cammi, *Chem. Rev.* **2005**, 105, 2999–3093
- (3) Gaussian 16, Revision A.03, M. J. Frisch, G. W. Trucks, H. B. Schlegel, G. E. Scuseria, M. A. Robb, J. R. Cheeseman, G. Scalmani, V. Barone, G. A. Petersson, H. Nakatsuji, X. Li, M. Caricato, A. V. Marenich, J. Bloino, B. G. Janesko, R. Gomperts, B. Mennucci, H. P. Hratchian, J. V. Ortiz, A. F. Izmaylov, J. L. Sonnenberg, D. Williams-Young, F. Ding, F. Lipparini, F. Egidi, J. Goings, B. Peng, A. Petrone, T. Henderson, D. Ranasinghe, V. G. Zakrzewski, J. Gao, N. Rega, G. Zheng, W. Liang, M. Hada, M. Ehara, K. Toyota, R. Fukuda, J. Hasegawa, M. Ishida, T. Nakajima, Y. Honda, O. Kitao, H. Nakai, T. Vreven, K. Throssell, J. A. Montgomery, Jr., J. E. Peralta, F. Ogliaro, M. J. Bearpark, J. J. Heyd, E. N. Brothers, K. N. Kudin, V. N. Staroverov, T. A. Keith, R. Kobayashi, J. Normand, K. Raghavachari, A. P. Rendell, J. C. Burant, S. S. Iyengar, J. Tomasi, M. Cossi, J. M. Millam, M. Klene, C. Adamo, R. Cammi, J. W. Ochterski, R. L. Martin, K. Morokuma, O. Farkas, J. B. Foresman, and D. J. Fox, Gaussian, Inc., Wallingford CT, 2016.
- (4) TURBOMOLE V6.6 2014, a development of University of Karlsruhe and Forschungszentrum Karlsruhe GmbH, 1989 – 2007, TURBOMOLE GmbH, since 2007; available from <http://www.turbomole.com>
- (5) R. Cammi, B. Mennucci, *J. Chem. Phys.* **1999**, 110, 9877–9886.
- (6) (a) R. Cammi, S. Corni, B. Mennucci, J. Tomasi, *J. Chem. Phys.* **2005**, 122, 104513; (b) M. Caricato, B. Mennucci, J. Tomasi, F. Ingrosso, R. Cammi, S. Corni, G. Scalmani, *J. Chem. Phys.* **2006**, 124, 124520.